Am J Transl Res 2020;12(11):7395-7403
www.ajtr.org /ISSN:1943-8141/AJTR0118848

Original Article

Plasma circular RNA panel acts as a novel diagnostic biomarker for colorectal cancer detection

Jipeng Li[1,2,3], Yulan Song[3], Jianhua Wang[3], Jian Huang[1,2]

[1]Department of Surgical Oncology, Second Affiliated Hospital, Zhejiang University School of Medicine, Hangzhou 310009, China; [2]Key Laboratory of Tumor Microenvironment and Immune Therapy of Zhejiang Province, Hangzhou 310009, China; [3]Department of Central Laboratory, The Affiliated People's Hospital of Ningbo University, Ningbo 315040, China

Received July 24, 2020; Accepted October 17, 2020; Epub November 15, 2020; Published November 30, 2020

Abstract: Circular RNAs (circRNAs) can function as key regulators of oncogenic processes, making them ideal diagnostic biomarkers of many cancers. However, few studies to date have reported on plasma circRNA profiles associated with colorectal cancer (CRC). To that end, we herein employed microarray- and qRT-PCR-based approaches to evaluate circulating plasma circRNAs in CRC patients. Area under the receiver operating characteristic curve (AUC) values were then used to assess the diagnostic utility of these circRNAs. We ultimately determined that hsa_circ_0001900, hsa_circ_0001178, and hsa_circ_0005927 were upregulated in the plasma of CRC patients relative to healthy controls and were correlated with clinicopathological findings in these patients. We further established that a panel composed of these three circRNAs (CircPanel) was able to differentiate between patients with and without CRC more reliably than CEA (carcinoembryonic antigen) (AUC, 0.859 [95% confidence interval, CI: 0.805-0.903] vs. 0.698 [0.631-0.759], *P*=0.0003), enabling us to detect patients with CEA-negative CRC. In conclusion, our study reveals that CircPanel could serve as a promising potential biomarker for CRC diagnosis.

Keywords: Circular RNAs, colorectal cancer, biomarker, plasma

Introduction

According to the latest statistics of the American Cancer Society in 2020, colorectal cancer ranks the third in the number of new cases and mortality [1]. While many advances in CRC patient diagnosis and treatment have been made in recent years, patient prognosis remains poor, with 5-year survival rates varying substantially depending upon the disease stage at the time of diagnosis [2].

Imaging and endoscopic approaches are the most common and effective means of reliably diagnosing CRC [3]. These strategies, however, are expensive and invasive, leading to poor patient compliance and making them ill-suited for CRC screening in high-risk patient groups [4]. Researchers have identified non-invasive biomarkers that can be employed to screen for CRC including a fecal occult blood test (FOBT) and measurements of carcinoembryonic antigen (CEA) levels, but the sensitivity and specificity of these two approaches remain somewhat limited [5, 6]. It is thus essential that novel non-invasive diagnostic biomarkers of CRC be identified to safely and effectively identify this disease during its earlier stages when it is more amenable to treatment.

Circular RNAs (circRNAs) are non-coding RNAs that form closed covalent loops lacking any 5' capping or 3'-poly (A) tailing [7, 8]. Owing to their unique structural properties, circRNAs are highly stable (>48 h half-life) and are highly conserved [9, 10], making them ideal potential diagnostic biomarkers of CRC and other cancers. Consistent with such promise, circulating circRNAs have been shown to be of diagnostic value in prior studies of lung cancer, hepatocellular carcinoma (HCC), and CRC [11-13]. He et al. determined that plasma exosome circRNA_0056616 levels were correlated with tumor grade and with lymph node metastasis in patients with lung adenocarcinoma, an area under the receiver operating characteristic (ROC) curve (AUC) analysis of this circRNA as a tool for diagnosing lymph node metastasis

yielding an AUC value of 0.812 (95% confidence interval [CI]: 0.720-0.903) with sensitivity and specificity values of 0.792 and 0.810, respectively [14]. Yin et al. employed a microarray-based approach to identify patterns of abnormal circRNA expression in the peripheral blood of breast cancer patients, leading them to identify hsa_circ_0001785 as a potentially valuable diagnostic biomarker in this cancer context [15]. Zhang et al. further determined that elevated plasma hsa_circ_0007534 levels in CRC patients were associated with tumor clinical classification, metastatic phenotype, and poor differentiation status [16].

Despite the above findings, the diagnostic value of circulating circRNAs in CRC remains poorly characterized. As such, we herein utilized microarray and qRT-PCR-based approaches in order to identify potential plasma circRNA biomarkers that may offer diagnostic utility in patients with CRC.

Materials and methods

Patients and samples

Samples utilized in this study were collected between 2017 and 2019 from patients at the Second Affiliated Hospital, Zhejiang University School of Medicine. CRC diagnosis was confirmed via pathological examination in appropriate patients. Healthy control samples were obtained from volunteers during routine physical examinations. Samples were stored at -80°C prior to use. For initial circRNA screening, plasma samples were collected from healthy controls and CRC patients (n=18 each), and tumor and matched paracancerous tissue samples were additionally collected from all 18 CRC patients. In addition, an independent validation cohort of plasma samples was collected that was comprised of samples from 80 healthy controls, 30 patients with precancerous lesions (colon adenomas and adenomatous polyps), and 102 CRC patients, including 20 patients from whom plasma was again collected 30 days following surgical tumor resection. The Ethics Committee of Second Affiliated Hospital, Zhejiang University School of Medicine approved this study, and patient clinicopathological characteristics are compiled in Table S1.

RNA preparation

TRIzol (Invitrogen, CA, USA) was used to extract RNA from tissue samples, while TRIzol™ LS (Invitrogen) was used to extract RNA from plasma samples based on provided directions. To enhance plasma RNA preparation, glycogen (ThermoFisher, final concentration: 100 μg/ml) was added during the isopropanol precipitation step. An ImProm-II Reverse Transcription System (Promega, WI, USA) was used based on provided instructions to prepare cDNA from extracted RNA.

Assessment of circRNA expression profiles

Initial microarray-based circRNA expression profiling was conducted by KangChen Biotech Company using plasma RNA samples prepared from CRC patients and healthy controls (n=3 each). Sample preparation and microarray hybridization were conducted according to provided directions (Arraystar, Inc). Briefly, samples were enriched for circRNAs by treating them with RNase R to degrade linear RNA, after which random primers were used to reverse transcribe enriched circRNAs into cDNA. Resultant labeled cDNAs were then hybridized onto an Arraystar human circRNA Array V2 (8×15 K), after which an Agilent Scanner G2505C was used to scan and analyze these arrays.

qRT-PCR

Power SYBR Green (Takara, Dalian, China) was used for qRT-PCR analyses of pairs of CRC and non-tumor tissues, with GAPDH used as a control for relative gene expression, which was assessed via the $2^{-\Delta\Delta Cq}$ method.

No endogenous control RNA has, to date, been established as a reliable endogenous control when quantifying plasma circRNA levels. In light of prior studies [12], we thus utilized an absolute quantification approach to measuring the expression levels of these circRNAs in patient plasma. Briefly, we cloned PCR products corresponding to the three circRNAs of interest into separate pcDNA3.0 vectors and diluted these constructs to between 1×10^5 and 1×10^2 copies/ml. These recombinant plasmids were then run under identical qRT-PCR conditions to those above in parallel with plasma RNA samples in order to construct appropriate standard curves (Figure S1), which were in turn used to quantify absolute circRNA levels within patient plasma samples. Primer sequences used in these analyses are listed in Table S2.

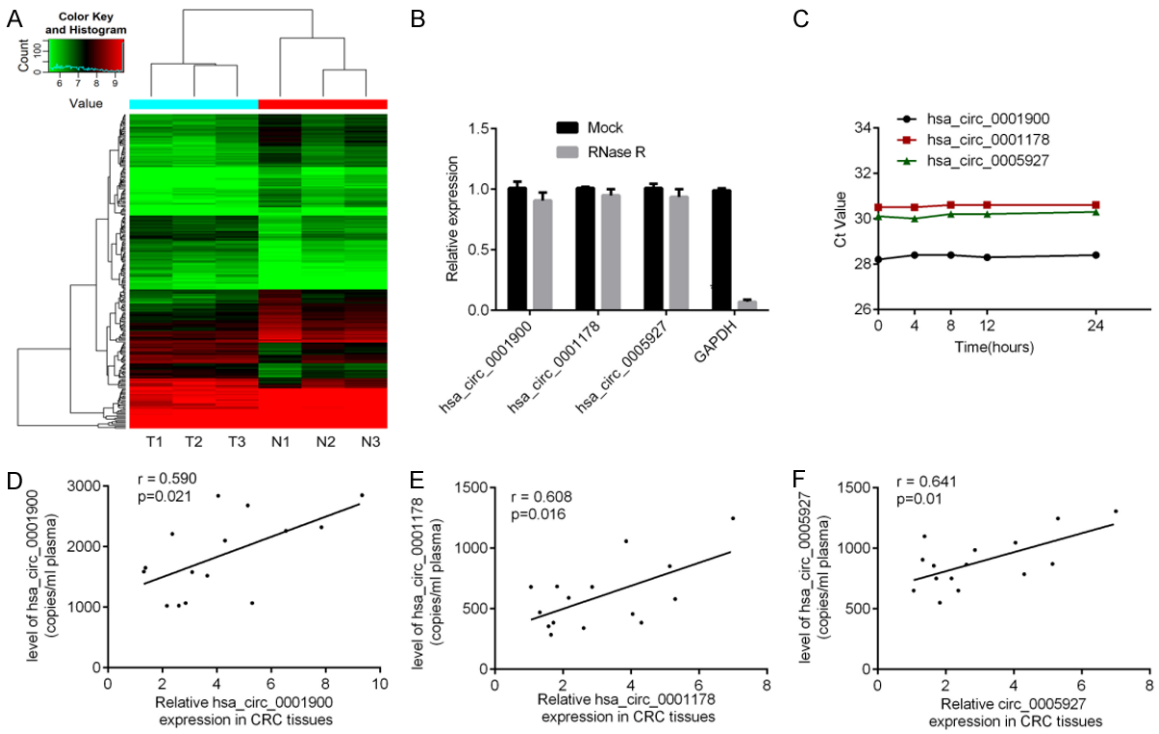

Figure 1. Candidate CRC-related circRNA identification. A. Differentially expressed circRNAs from the plasma of CRC patients and healthy controls (n=3) were subjected to hierarchical clustering analysis. B. qRT-PCR analysis of RNase R-resistant circRNAs, with GAPDH serving as a negative control. C. No changes in Ct values for these three circRNAs were detected following a 24 h incubation at room temperature, as measured via qRT-PCR. D-F. Correlations between plasma and intratumoral levels of these differentially expressed circRNAs in CRC patients (n=15).

Statistical analysis

SPSS 22.0 (SPSS, Inc., IL, USA) and GraphPad Prism 7.0 (GraphPad, Inc., CA, USA) were used for statistical testing. Data were compared using Student's t-tests and Man-Whitney tests, as appropriate. Pearson's correlation analyses were employed to assess relationships between variables. The CircPanel diagnostic model was developed through binary logistic regression analyses. ROC curve analyses were used to determine optimal plasma circRNA expression cutoff values in order to maximize diagnostic utility after using MedCalc 11.0 (MedCalc, Ostend, Belgium) to generate ROC curves. $P<0.05$ was the significance threshold in these analyses.

Results

Identification of CRC-related plasma circRNA expression profiles

We began by employing a microarray approach in order to detect circRNAs that were differentially expressed in the plasma of CRC patients and healthy controls. In total, we identified 226 circRNAs exhibiting >1.5-fold expression level differences between these two patient cohorts, including 88 and 138 that were up- and down-regulated, respectively (**Figure 1A**; Table S3). We then compared the 88 identified upregulated circRNAs with a previous dataset evaluating differential circRNA expression profiles in CRC patient tissues [17-19], leading us to identify six potential CRC-related candidate circRNAs (hsa_circ_0001900, hsa_circ_0036005, hsa_circ_0067185, hsa_circ_0005075, hsa_circ_0001178, and hsa_circ_0005927). Of these, we were able to confirm that three (hsa_circ_0001900, hsa_circ_0001178, and hsa_circ_0005927) were significantly differentially expressed in CRC patient plasma and CRC tumor tissues via qRT-PCR and Sanger sequencing (Figure S2A-C). We further confirmed that these putative circRNAs were RNase R-resistant, indicating that they adopt a circular rather than linear conformation (**Figure 1B**). We additionally found that these circRNAs did not undergo significant degradation when plasma

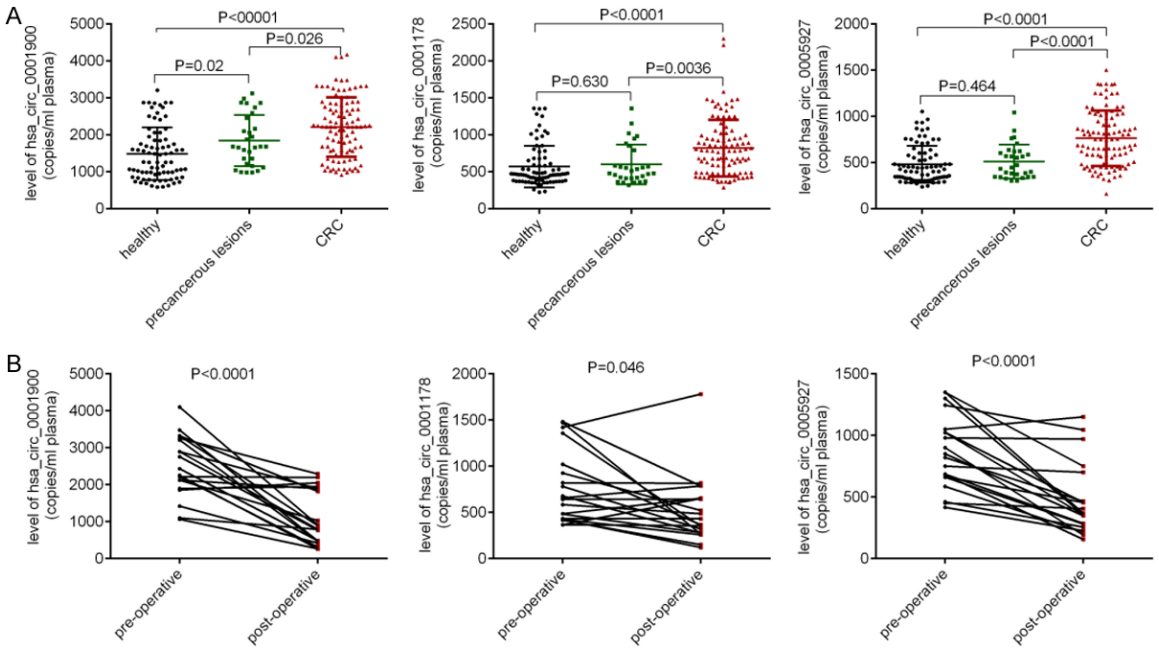

Figure 2. Validation of candidate CRC-related circulating circRNA profiles in an independent patient cohort. A. Levels of hsa_circ_0001900, hsa_circ_0001178, and hsa_circ_0005927 were assessed in the plasma of 102 CRC patients, 42 healthy controls, and 30 patients with precancerous lesions via qRT-PCR. B. Levels of hsa_circ_0001900, hsa_circ_0001178, and hsa_circ_0005927 were assessed via qRT-PCR in 20 paired plasma samples from CRC patients before and after surgery.

was stored at room temperature for 24 h (**Figure 1C**), confirming that they are highly stable in this biological matrix. We further found that hsa_circ_0001900, hsa_circ_0001178, and hsa_circ_0005927 expression levels in CRC tissues were positively correlated with levels in patient plasma (**Figure 1D-F**), suggesting that these circRNAs may be secreted from tumors into circulation.

Independent validation of candidate CRC-related circRNA expression profiles

To validate the clinical relevance of hsa_circ_0001900, hsa_circ_0001178, and hsa_circ_0005927 in the context of CRC, we next evaluated the expression of these circRNAs in plasma samples from 42 healthy controls, 30 patients with precancerous lesions, and 102 CRC patients. Furthermore pre- and post-operative plasma samples from 20 of the CRC patients were additionally compared in these analyses. We found that hsa_circ_0001900, hsa_circ_0001178, and hsa_circ_0005927 were all expressed at significantly higher levels in the plasma of CRC patients relative to levels in the plasma of healthy controls of patients with precancerous lesions ($P<0.05$, **Figure 2A**). We also found that hsa_circ_0001900 was differentially expressed when comparing plasma samples from healthy controls to those from patients with precancerous lesions ($P=0.02$, **Figure 2A**). We also found that the plasma levels of these three circRNAs decreased significantly in CRC patients following surgical tumor resection (**Figure 2B**). AS such, our findings strongly suggest that hsa_circ_0001900, hsa_circ_0001178, and hsa_circ_0005927 are primarily derived from tumor cells in CRC patients.

Correlations between candidate circRNA expression levels and CRC patient clinical characteristics

We next assess correlations between plasma levels of these three candidate circRNAs and clinicopathological findings in 102 CRC patients. In so doing, we found that hsa_circ_0001900 was correlated with tumor size ($P=0.017$), TNM stage ($P=0.005$), lymph node metastasis ($P=0.013$), and distant metastasis ($P<0.0001$), while hsa_circ_0001178 was associated with lymph node metastasis ($P=0.0012$) and distant metastasis ($P=0.023$), and hsa_circ_0005927 was correlated with tumor size ($P=0.0006$). None of these circRNAs

Table 1. Association between candidate circRNAs expression and clinicopathological characteristics

Characteristics	Cases (n=102)	hsa_circ_0001900		hsa_circ_0001178		hsa_circ_0005927	
		Mean ± SD	*P*	Mean ± SD	P	Mean ± SD	*P*
Age			0.182		0.909		0.194
<65	41	2076 ± 127.8		816.5 ± 74.3		798.5 ± 51.0	
≥65	61	2293 ± 101.0		825.4 ± 39.9		881.1 ± 38.3	
Gender			0.810		0.712		0.489
Male	62	2190 ± 98.7		831.7 ± 39.9		863.1 ± 46.5	
Female	40	2230 ± 134.8		802.8 ± 75.3		820.5 ± 39.8	
Tumor site			0.857		0.156		0.390
Colon	50	2191 ± 115.3		768.4 ± 56.3		886.3 ± 49.3	
Rectum	52	2220 ± 111.0		876.6 ± 49.9		829.0 ± 44.2	
Tumor size (cm)			0.017		0.082		0.0006
<5	68	2072 ± 92.6		881.0 ± 45.8		774.6 ± 32.7	
≥5	34	2471 ± 141.9		741.1 ± 65.4		994.5 ± 58.5	
TNM stage			0.005		0.513		0.073
I+II	54	1999 ± 100.5		796.8 ± 42.3		795.8 ± 40.7	
III+IV	48	2438 ± 118.1		846.9 ± 65.5		906.6 ± 45.9	
Lymphatic metastasis			0.013		0.0012		0.162
Postive	47	2418 ± 119.8		932.3 ± 54.0		888.0 ± 44.7	
Negative	55	2024 ± 101.0		689.4 ± 46.8		801.9 ± 41.5	
Distal metastasis			<0.0001		0.023		0.163
Yes	14	2981 ± 203.7		1037 ± 126.2		956.1 ± 89.7	
No	88	2082 ± 79.1		786.0 ± 38.3		830.7 ± 32.6	

were correlated with characteristics such as age, sex, or tumor site (**Table 1**).

Assessment of the diagnostic utility of the three identified candidate circRNAs in CRC

We next gauged the diagnostic value of these three circRNAs using ROC curves. When distinguishing between CRC and non-CRC patient samples, we found that AUC values for hsa_circ_0001900, hsa_circ_0001178, and hsa_circ_0005927 were 0.722 (95% CI: 0.656-0.781), 0.718 (95% CI: 0.652-0.778), and 0.784 (95% CI: 0.722-0.837), respectively (**Figure 3A-C**). We then employed a binary logistic regression analysis in order to construct a diagnostic model incorporating all three of these circRNAs (CircPanel). The AUC, sensitivity, and specificity of CircPanel when distinguishing between CRC and non-CRC patient samples were 0.859 (95% CI: 0.805-0.903), 72.55%, and 82.73%, respectively, with these values being substantially higher than values for any individual circRNA (**Figure 3D**; Table S4). As such, we elected to focus on the diagnostic utility of CircPanel for the remainder of this study.

The diagnostic performance of CircPanel and/or CEA in the detection of CRC

We next evaluated the relative value of CircPanel, the CRC protein biomarker CEA, or a combination of these two biomarkers (CircPanel+CEA) as tools for diagnosing CRC. We found that both CircPanel alone and CircPanel+CEA were more accurate than CEA alone as a means of differentiating between CRC and non-CRC patient samples (CircPanel vs. CEA: AUC 0.859 [0.805-0.903] vs. AUC 0.698 [0.631-0.759], P=0.0003); (CircPanel+CEA vs. CEA: AUC 0.881 [0.829-0.921] vs. AUC 0.698 [0.631-0.759], P<0.0001). However, we did not detect any significant differences in the relative abilities of CircPanel and CircPanel+CEA to differentiate between CRC and non-CRC patient samples (**Figure 4A**; **Table 2**). We further subdivided non-CRC patient samples into samples from healthy controls and samples from patients with precancerous lesions, and observed similar results when comparing samples from CRC patients and samples from patients with precancerous lesions (**Figure 4B**; **Table 2**). We also found that the diagnostic performance of

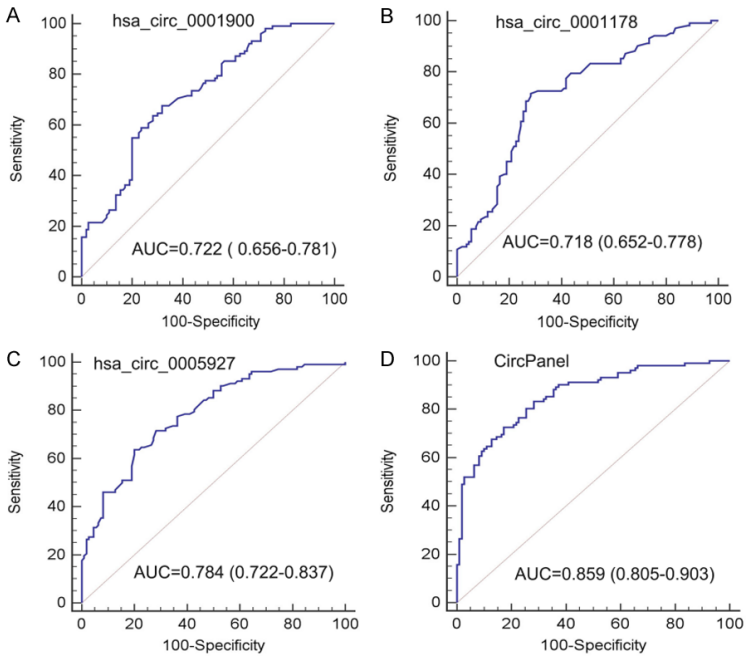

Figure 3. The diagnostic potential for three candidate circRNAs and the combination thereof as a means of differentiating between CRC and non-CRC patient samples. A. ROC curve corresponding to hsa_circ_0001900. B. ROC curve corresponding to hsa_circ_0001178. C. ROC curve corresponding to hsa_circ_0005927. D. ROC corresponding to the overall CircPanel.

CircPanel+CEA was superior to that of CircPanel alone as a means of differentiating between CRC patients and healthy controls (circPanel+CEA vs. CircPanel: AUC: 0.903 [0.860-0.947] vs. AUC 0.874 [0.816-0.918], *P*=0.0014) (**Figure 4C**; **Table 2**).

CircPanel can effectively diagnose CEA-negative CRC

There is some clinical evidence that serum CEA positivity rates in CRC patients may be <50% [5]. As such, we specifically evaluated the ability of CircPanel to diagnose CEA-negative (<5 ng/ml) CRC. Overall, CircPanel achieved high diagnostic accuracy when differentiating between CRC and non-CRC patient samples, between CRC and precancerous samples, and between CRC and healthy samples that were CEA-negative (all AUCs >0.800; **Figure 5**; Table S5). These findings thus show that CircPanel may be a valuable biomarker that can be used to diagnose patients with CEA-negative CRC.

Discussion

Many studies to date have confirmed that circRNA dysregulation is closely linked to tumor development and progression in a range of tissue and cell types [20, 21]. Many circRNAs can be stably detected in human peripheral blood under physiological and pathological conditions, making them ideal tumor biomarkers [22-24]. To evaluate the potential diagnostic utility of such circRNAs in the context of CRC, we employed a microarray-based approach that led us to detect 88 and 138 circRNAs that were up- and down-regulated in the plasma of CRC patients, respectively, when compared to the plasma of healthy control patients. After combining these data with published tissue circRNA profiles, we identified three circRNAs (hsa_circ_0001900, hsa_circ_0001178, and hsa_circ_0005927) as being ideal diagnostic candidates for the detection of CRC.

Recent studies have revealed that hsa_circ_0001900 and hsa_circ_0001178 are significantly increased in CRC tissues and correlated with poor prognosis of CRC patients [17, 19]. Hsa_circ_0001900 acts as the sponge of miR-328-5p to promote CRC growth, while hsa_circ_0001178 facilitates CRC metastasis by upregulating transcription factors ZEB1. To date, the role of hsa_circ_0005927 in tumor is still unknown. In this study, ROC curve analysis was performed to evaluate the diagnostic value of the three plasma circRNAs in distinguishing CRC from non-CRC. The results showed AUC values for hsa_circ_0001900, hsa_circ_0001178, and hsa_circ_0005927 were 0.722, 0.718 and 0.784, respectively, indicating that the three circRNAs have certain diagnostic value for CRC.

Following logistic regression analyses, we established a CircPanel composed of these three circRNAs that we found to be more accurate than any of these individual circRNAs as a tool for differentiating between CRC and non-CRC patient samples. Non-CRC patient samples were further subdivided into those from healthy controls and those from patients with precancerous lesions. We found that analyzing a combination of plasma CircPanel expression and CEA levels (CircPanel+CEA) was sufficient

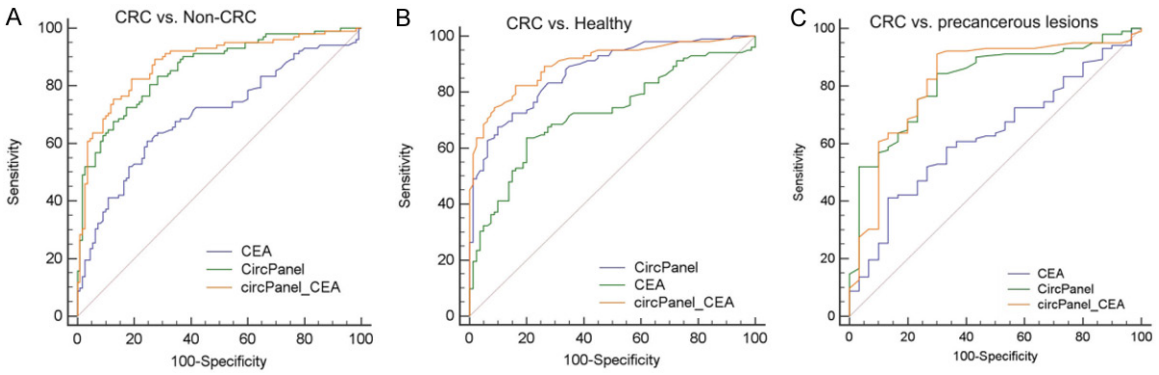

Figure 4. Assessment of the diagnostic utility of CircPanel, CEA, and the combination thereof. A. ROC curve analysis of the ability to differentiate between CRC and non-CRC patient samples. B. ROC curve analysis of the ability to differentiate between CRC and healthy patient samples. C. ROC curve of the ability to differentiate between samples from patients with CRC and patients with precancerous lesions.

Table 2. The performance of CircPanel, CEA and their combination for the diagnosis of CRC

Groups	AUC (95% CI)	Sensitivity (%)	Specificity (%)	Comparation of AUC	
				Groups	*P* value
CRC vs. Non-CRC					
circPanel	0.859 (0.805-0.903)	72.55	82.73	circPanel vs. CEA	0.0003
CEA	0.698 (0.631-0.759)	60.78	75.45	circPanel+CEA vs. CEA	<0.0001
circPanel+CEA	0.881 (0.829-0.921)	82.35	80.91	circPanel vs. circPanel+CEA	0.095
CRC vs. Healthy					
circPanel	0.874 (0.816-0.918)	67.65	90.00	circPanel vs. CEA	0.0014
CEA	0.724 (0.653-0.788)	63.73	80.00	circPanel+CEA vs. CEA	<0.0001
circPanel+CEA	0.903 (0.851-0.942)	82.35	83.75	circPanel vs. circPanel+CEA	0.0092
CRC vs. precancerous lesions					
circPanel	0.818 (0.741-0.880)	84.31	70.00	circPanel vs. CEA	0.0037
CEA	0.626 (0.538-0.709)	41.18	86.67	circPanel+CEA vs. CEA	0.0002
circPanel+CEA	0.820 (0.744-0.881)	91.18	70.00	circPanel vs. circPanel+CEA	0.9404

to more effectively differentiate between CRC patients and healthy controls. However, we did not detect any differences in the ability of CircPanel+CEA and CircPanel alone to differentiate between CRC and non-CRC samples or CRC samples and samples from patients with precancerous lesions. Importantly, CircPanel alone exhibited robust diagnostic utility as a means of differentiating between CEA-negative CRC patient plasma samples and non-CRC patient plasma samples. Together, these findings underscore the utility of CircPanel as an ideal non-invasive diagnostic biomarker for the detection of CRC.

Herein, we further observed no significant differences in the expression of hsa_circ_0036005, hsa_circ_0067185, or hsa_circ_0005075, which are expressed at high levels in CRC tumor tissues, in CRC patient plasma relative to healthy control patient plasma (data not shown). Yu et al. have previously demonstrated that while hsa_circ_0139897 expression did not differ significantly between HCC patient tumor and paracancerous tissues, following tumor resection the plasma levels of this circRNA in HCC patients declined significantly [12]. Prior studies have also shown that circCCDC66 and circ-STIL upregulation occurs in CRC patient tissues, driving the proliferative and invasive activities of these tumor cells [25-27]. In contrast, Lin et al. found these two circRNAs to be downregulated in CRC patient plasma samples [11]. Together these findings emphasize that circulating circRNAs are likely secreted in a specific manner, although the mechanisms governing such specific circRNA secretion remain to be clarified.

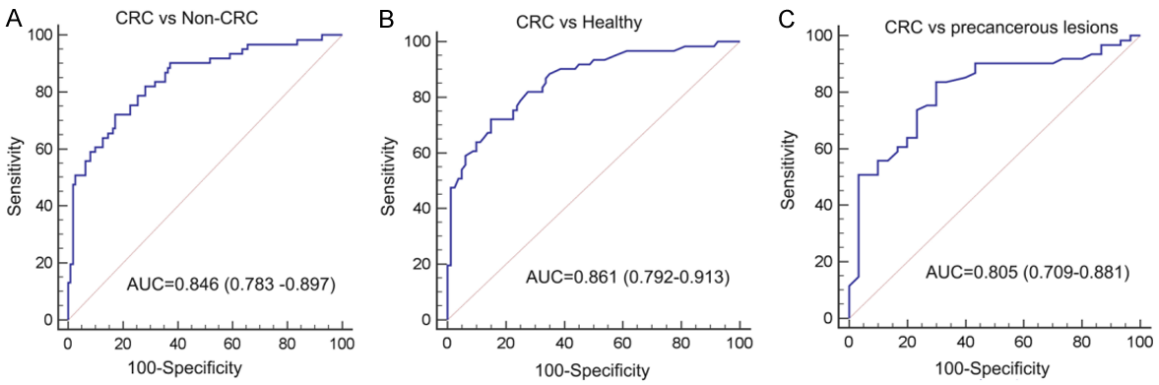

Figure 5. The utility of CircPanel as a means of diagnosing CEA-negative CRC. A. ROC curve assessment for CircPanel-mediated differentiation between CRC and non-CRC samples. B. ROC curve assessment for CircPanel-mediated differentiation between CRC and healthy patient samples. C. ROC curve assessment for CircPanel-mediated differentiation between patients with CRC and patients with precancerous lesions.

In conclusion, in the present study we identified a panel of three circRNAs (hsa_circ_0001900, hsa_circ_0001178 and hsa_circ_0005927) that are differentially expressed in CRC patient plasma, and that therefore represent viable diagnostic biomarkers for the detection of this deadly form of cancer.

Acknowledgements

This work was supported by the National Natural Science Foundation of China (NO. 81930079 and 31471391).

Disclosure of conflict of interest

None.

Address correspondence to: Jian Huang, Department of Surgical Oncology, Second Affiliated Hospital, Zhejiang University School of Medicine, Hangzhou 310009, China. E-mail: drhuangjian@zju.edu.cn

References

[1] Siegel RL, Miller KD and Jemal A. Cancer statistics, 2020. CA Cancer J Clin 2020; 70: 7-30.

[2] Dienstmann R, Vermeulen L, Guinney J, Kopetz S, Tejpar S and Tabernero J. Consensus molecular subtypes and the evolution of precision medicine in colorectal cancer. Nat Rev Cancer 2017; 17: 79-92.

[3] ASGE Standards of Practice Committee, Fisher DA, Shergill AK, Early DS, Acosta RD, Chandrasekhara V, Chathadi KV, Decker GA, Evans JA, Fanelli RD, Foley KQ, Fonkalsrud L, Hwang JH, Jue T, Khashab MA, Lightdale JR, Muthusamy VR, Pasha SF, Saltzman JR, Sharaf R and Cash BD. Role of endoscopy in the staging and management of colorectal cancer. Gastrointest Endosc 2013; 78: 8-12.

[4] Garborg K, Holme O, Loberg M, Kalager M, Adami HO and Bretthauer M. Current status of screening for colorectal cancer. Ann Oncol 2013; 24: 1963-1972.

[5] Duffy MJ, van Dalen A, Haglund C, Hansson L, Klapdor R, Lamerz R, Nilsson O, Sturgeon C and Topolcan O. Clinical utility of biochemical markers in colorectal cancer: European Group on Tumour Markers (EGTM) guidelines. Eur J Cancer 2003; 39: 718-727.

[6] Zauber AG, Lansdorp-Vogelaar I, Knudsen AB, Wilschut J, van Ballegooijen M and Kuntz KM. Evaluating test strategies for colorectal cancer screening: a decision analysis for the U.S. Preventive Services Task Force. Ann Intern Med 2008; 149: 659-669.

[7] Barrett SP and Salzman J. Circular RNAs: analysis, expression and potential functions. Development 2016; 143: 1838-1847.

[8] Chen LL and Yang L. Regulation of circRNA biogenesis. RNA Biol 2015; 12: 381-388.

[9] Jeck WR, Sorrentino JA, Wang K, Slevin MK, Burd CE, Liu J, Marzluff WF and Sharpless NE. Circular RNAs are abundant, conserved, and associated with ALU repeats. RNA 2013; 19: 141-157.

[10] Memczak S, Papavasileiou P, Peters O and Rajewsky N. Identification and characterization of circular RNAs as a new class of putative biomarkers in human blood. PLoS One 2015; 10: e0141214.

[11] Lin J, Cai D, Li W, Yu T, Mao H, Jiang S and Xiao B. Plasma circular RNA panel acts as a novel diagnostic biomarker for colorectal cancer. Clin Biochem 2019; 74: 60-68.

[12] Yu J, Ding WB, Wang MC, Guo XG, Xu J, Xu QG, Yang Y, Sun SH, Liu JF, Qin LX, Liu H, Yang F

and Zhou WP. Plasma circular RNA panel to diagnose hepatitis B virus-related hepatocellular carcinoma: a large-scale, multicenter study. Int J Cancer 2020; 146: 1754-1763.

[13] Zhu X, Wang X, Wei S, Chen Y, Chen Y, Fan X, Han S and Wu G. hsa_circ_0013958: a circular RNA and potential novel biomarker for lung adenocarcinoma. FEBS J 2017; 284: 2170-2182.

[14] He F, Zhong X, Lin Z, Lin J, Qiu M, Li X and Hu Z. Plasma exo-hsa_circRNA_0056616: a potential biomarker for lymph node metastasis in lung adenocarcinoma. J Cancer 2020; 11: 4037-4046.

[15] Yin WB, Yan MG, Fang X, Guo JJ, Xiong W and Zhang RP. Circulating circular RNA hsa_circ_0001785 acts as a diagnostic biomarker for breast cancer detection. Clin Chim Acta 2018; 487: 363-368.

[16] Zhang W, Yang S, Liu Y, Wang Y, Lin T, Li Y and Zhang R. Hsa_circ_0007534 as a blood-based marker for the diagnosis of colorectal cancer and its prognostic value. Int J Clin Exp Pathol 2018; 11: 1399-1406.

[17] Ren C, Zhang Z, Wang S, Zhu W, Zheng P and Wang W. Circular RNA hsa_circ_0001178 facilitates the invasion and metastasis of colorectal cancer through upregulating ZEB1 via sponging multiple miRNAs. Biol Chem 2020; 401: 487-496.

[18] Tian Y, Xu Y, Wang H, Shu R, Sun L, Zeng Y, Gong F, Lei Y, Wang K and Luo H. Comprehensive analysis of microarray expression profiles of circRNAs and lncRNAs with associated co-expression networks in human colorectal cancer. Funct Integr Genomics 2019; 19: 311-327.

[19] Zhou C, Liu HS, Wang FW, Hu T, Liang ZX, Lan N, He XW, Zheng XB, Wu XJ, Xie D, Wu XR and Lan P. circCAMSAP1 promotes tumor growth in colorectal cancer via the miR-328-5p/E2F1 axis. Mol Ther 2020; 28: 914-928.

[20] Liu J, Li D, Luo H and Zhu X. Circular RNAs: the star molecules in cancer. Mol Aspects Med 2019; 70: 141-152.

[21] Tu FL, Guo XQ, Wu HX, He ZY, Wang F, Sun AJ and Dai XD. Circ-0001313/miRNA-510-5p/AKT2 axis promotes the development and progression of colon cancer. Am J Transl Res 2020; 12: 281-291.

[22] Lei B, Zhou J, Xuan X, Tian Z, Zhang M, Gao W, Lin Y, Ni B, Pang H and Fan W. Circular RNA expression profiles of peripheral blood mononuclear cells in hepatocellular carcinoma patients by sequence analysis. Cancer Med 2019; 8: 1423-1433.

[23] Li Y, Zheng Q, Bao C, Li S, Guo W, Zhao J, Chen D, Gu J, He X and Huang S. Circular RNA is enriched and stable in exosomes: a promising biomarker for cancer diagnosis. Cell Res 2015; 25: 981-984.

[24] Mu Y, Xie F, Huang Y, Yang D, Xu G, Wang C and Wu Q. Circular RNA expression profile in peripheral whole blood of lung adenocarcinoma by high: throughput sequencing. Medicine (Baltimore) 2019; 98: e17601.

[25] Guo JN, Li J, Zhu CL, Feng WT, Shao JX, Wan L, Huang MD and He JD. Comprehensive profile of differentially expressed circular RNAs reveals that hsa_circ_0000069 is upregulated and promotes cell proliferation, migration, and invasion in colorectal cancer. Onco Targets Ther 2016; 9: 7451-7458.

[26] Hsiao KY, Lin YC, Gupta SK, Chang N, Yen L, Sun HS and Tsai SJ. Noncoding effects of circular RNA CCDC66 promote colon cancer growth and metastasis. Cancer Res 2017; 77: 2339-2350.

[27] Wang L, Peng X, Lu X, Wei Q, Chen M and Liu L. Inhibition of hsa_circ_0001313 (circCCDC66) induction enhances the radio-sensitivity of colon cancer cells via tumor suppressor miR-338-3p: effects of cicr_0001313 on colon cancer radio-sensitivity. Pathol Res Pract 2019; 215: 689-696.

Table S1. Clinicopathological characteristics of the patients in the screening and validation cohorts

	Screening cohort		*P*	Validation cohort			*P*
	CRC (n=18)	Control (n=18)		CRC (n=102)	Healthy (n=80)	Precancerous lesions (n=30)	
Age (Mean ± SD)	65.01 ± 10.22	64.81 ± 9.05	0.861	65.83 ± 9.45	63.01 ± 9.81	64.32 ± 8.79	0.902
Gender n (%)							
Male	11 (61.11)	11 (61.11)	1	62 (60.78)	45 (56.25)	18 (60.00)	0.916
Female	7 (38.89)	7 (38.89)		40 (39.22)	35 (43.75)	12 (40.00)	
Tumor site n (%)							
Colon				50 (49.02)			
Rectum				52 (50.98)			
Tumor size (cm) n (%)							
<5				68 (66.67)			
≥5				34 (33.33)			
TNM stage n (%)							
I+II				54 (52.94)			
III+IV				48 (47.06)			
Lymphatic metastasis n (%)							
Postive				47 (46.08)			
Negative				55 (53.92)			
Distal metastasis n (%)							
Yes				14 (13.23)			
No				88 (86.77)			
CEA n (%)							
<5 ng/ml				61 (59.80)			
≥5 ng/ml				41 (40.20)			

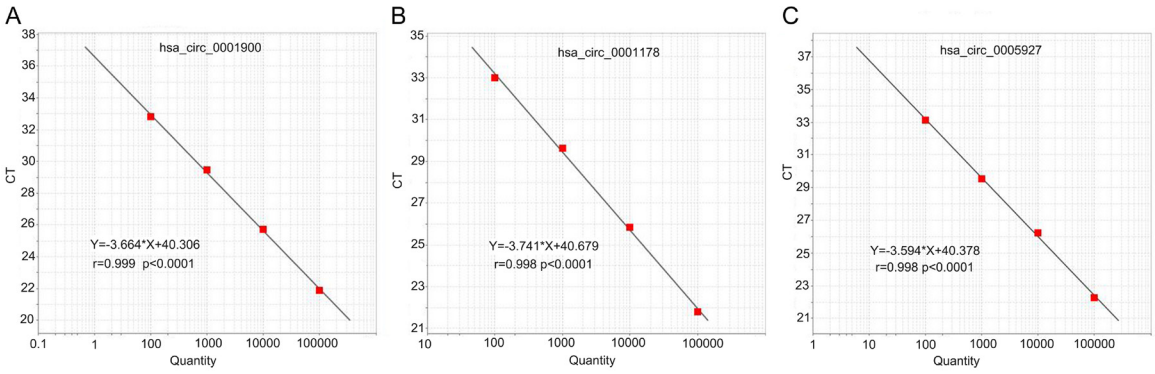

Figure S1. The standard curves used in the absolute quantitation experiments. A. The standard curve of hsa_circ_0001900. B. The standard curve of hsa_circ_0001178. C. The standard curve of hsa_circ_0005927.

Table S2. Primer sequences for real-time PCR

Primers for PCR	5'–>3'
hsa_circ_0036005-F	CACTGAAACGGAGGCTACCA
hsa_circ_0036005-R	TCGGACAGATCCAGTGGCTT
hsa_circ_0001900-F	AGTGCCTCGAAAGAACTTC
hsa_circ_0001900-R	TCCTGCTCATACTGGTCAA
hsa_circ_0001178-F	GTGTGGGAAGCCAAGCAG
hsa_circ_0001178-R	GGGTGTCATTAATCCCCG
hsa_circ_0067185-F	AAGGTCCTTGCTGCGAAAGTG
hsa_circ_0067185-R	GGCTCCATGGGACACAAAGAT
hsa_circ_0005075-F	GGGGCATCCAAATCTTGCG
hsa_circ_0005075-R	GAGACAGCGGGAGTGAAGAT
hsa_circ_0005927-F	CCGTTTTGGCATTGCTGCTA
hsa_circ_0005927-R	GCCATAGATGGTTGGTCCAGA
GAPDH-F	CAATGACCCCTTCATTGACC
GAPDH-R	TTGATTTTGGAGGGATCTCG

Table S3. The circRNAs expression profiles difference in plasma between CRC and healthy individuals

circRNA	Alias	chrom	circRNA_type	GeneSymbol	*P*-value	FDR	FC (abs)	Regulation
hsa_circRNA_007084	hsa_circ_0007084	chr10	exonic	MLLT10	0.036117044	0.499615783	5.83982	up
hsa_circRNA_017854	hsa_circ_0017854	chr10	exonic	PTER	0.046143326	0.499615783	4.4675495	up
hsa_circRNA_103981	hsa_circ_0074428	chr5	exonic	RBM27	0.046458938	0.499615783	4.2218987	up
hsa_circRNA_001754	hsa_circ_0000559	chr14	exonic	FOXN3	0.025503925	0.499615783	4.1709265	up
hsa_circRNA_104600	hsa_circ_0005927	Chr8	exonic	VDAC3	0.024185631	0.499615783	4.0418631	up
hsa_circRNA_103297	hsa_circ_0064416	chr3	exonic	HDAC11	0.027854528	0.499615783	4.0412256	up
hsa_circRNA_102896	hsa_circ_0057805	chr2	exonic	BMPR2	0.020588147	0.499615783	4.036511	up
hsa_circRNA_003792	hsa_circ_0003792	chr12	exonic	CACNA1C	0.046955987	0.499615783	3.9723317	up
hsa_circRNA_104962	hsa_circ_0001900	Chr9	exonic	CAMSAP1	0.00301487	0.499615783	3.5432527	up
hsa_circRNA_101571	hsa_circ_0036005	chr15	exonic	SMAD6	0.034117193	0.499615783	3.1165133	up
hsa_circRNA_104429	hsa_circ_0081308	chr7	exonic	TRRAP	0.022167581	0.499615783	2.8667034	up
hsa_circRNA_406399		chr3	intergenic		0.031250733	0.499615783	2.861345	up
hsa_circRNA_101950	hsa_circ_0041501	chr17	exonic	ZZEF1	0.001697309	0.499615783	2.8198155	up
hsa_circRNA_104889	hsa_circ_0005456	chr9	exonic	PAPPA	0.038631094	0.499615783	2.804286	up
hsa_circRNA_023787	hsa_circ_0023787	chr11	exonic	ALG8	0.046045444	0.499615783	2.8031158	up
hsa_circRNA_101873	hsa_circ_0004315	chr16	exonic	GLG1	0.037201761	0.499615783	2.7926335	up
hsa_circRNA_104893	hsa_circ_0008792	chr9	exonic	PAPPA	0.018998473	0.499615783	2.7834134	up
hsa_circRNA_104860	hsa_circ_0003965	chr9	exonic	TMEM245	0.025080796	0.499615783	2.7831586	up
hsa_circRNA_404823		chr10	exonic	FAM196A	0.027641439	0.499615783	2.6741565	up
hsa_circRNA_103112	hsa_circ_0001178	Chr21	exonic	USP25	0.033223211	0.499615783	2.6721098	up
hsa_circRNA_103461	hsa_circ_0067185	Chr3	exonic	MGLL	0.031738425	0.499615783	2.4310559	up
hsa_circRNA_024524	hsa_circ_0024524	chr11	exonic	VPS11	0.048332872	0.499615783	2.4210662	up
hsa_circRNA_405612		chr17	exonic	BRIP1	0.023930274	0.499615783	2.4062464	up
hsa_circRNA_005752	hsa_circ_0005752	chr9	intronic	LPAR1	0.028415502	0.499615783	2.2929431	up
hsa_circRNA_100457	hsa_circ_0000184	chr1	exonic	KCTD3	0.04574991	0.499615783	2.2870281	up
hsa_circRNA_406140		chr21	exonic	TMEM50B	0.045890997	0.499615783	2.2862256	up
hsa_circRNA_401530		chr16	exonic	PPL	0.012100874	0.499615783	2.2847012	up
hsa_circRNA_054272	hsa_circ_0054272	chr2	exonic	MTA3	0.015505573	0.499615783	2.2827146	up
hsa_circRNA_100085	hsa_circ_0005075	Chr1	exonic	EIF4G3	0.007403052	0.499615783	2.178074	up
hsa_circRNA_006341	hsa_circ_0006341	chr20	exonic	ATP9A	0.022098283	0.499615783	2.1747313	up
hsa_circRNA_103601	hsa_circ_0002515	chr4	exonic	AFAP1	0.02865817	0.499615783	1.6698874	up
hsa_circRNA_029545	hsa_circ_0029545	chr12	exonic	PGAM5	0.027418205	0.499615783	1.6692839	up
hsa_circRNA_001175	hsa_circ_0001658	chr6	exonic	ARID1B	0.035059236	0.499615783	1.6671372	up
hsa_circRNA_400011	hsa_circ_0092374	chr1	intronic	GADD45A	0.027357274	0.499615783	1.6629164	up

hsa_circRNA_000265	hsa_circ_0000265	chr10	intronic	RP11-12J10.3	0.028460833	0.499615783	1.6582831	up
hsa_circRNA_061107	hsa_circ_0061107	chr20	exonic	RPS21	0.049681123	0.499615783	1.6568239	up
hsa_circRNA_092558	hsa_circ_0001594	chr6	sense overlapping	HIST1H2AJ	0.015893142	0.499615783	1.6488262	up
hsa_circRNA_103371	hsa_circ_0002023	chr3	exonic	CDC25A	0.018866699	0.499615783	1.6481547	up
hsa_circRNA_406454		chr4	exonic	LCORL	0.025460645	0.499615783	1.6460056	up
hsa_circRNA_104660	hsa_circ_0085061	chr8	exonic	VPS13B	0.035703592	0.499615783	1.6456559	up
hsa_circRNA_100920	hsa_circ_0023919	chr11	exonic	PICALM	0.03429268	0.499615783	1.6453489	up
hsa_circRNA_405930		chr2	intronic	SNRNP200	0.049886147	0.499615783	1.6436896	up
hsa_circRNA_033191	hsa_circ_0033191	chr14	exonic	WARS	0.032660642	0.499615783	1.6387122	up
hsa_circRNA_092488	hsa_circ_0001058	chr2	exonic	RNF149	0.024797164	0.499615783	1.6289102	up
hsa_circRNA_001442	hsa_circ_0001442	chr4	exonic	SETD7	0.037862648	0.499615783	1.6230007	up
hsa_circRNA_020094	hsa_circ_0020094	chr10	exonic	ATRNL1	0.03459415	0.499615783	1.6205349	up
hsa_circRNA_102043	hsa_circ_0043244	chr17	exonic	ACACA	0.00586774	0.499615783	1.6136041	up
hsa_circRNA_104067	hsa_circ_0002245	chr6	exonic	CAP2	0.027429502	0.499615783	1.613415	up
hsa_circRNA_006823	hsa_circ_0006823	chr17	exonic	MLX	0.015731237	0.499615783	1.612977	up
hsa_circRNA_104568	hsa_circ_0002075	chr8	exonic	BMP1	0.031510323	0.499615783	1.6121542	up
hsa_circRNA_080302	hsa_circ_0080302	chr7	exonic	CCT6P3	0.044175246	0.499615783	1.6056281	up
hsa_circRNA_104771	hsa_circ_0002702	chr9	exonic	RUSC2	0.047751597	0.499615783	1.6028586	up
hsa_circRNA_000786	hsa_circ_0000786	chr17	exonic	DGKE	0.005520226	0.499615783	1.6020036	up
hsa_circRNA_100800	hsa_circ_0021773	chr11	exonic	TTC17	0.04384933	0.499615783	1.5896907	up
hsa_circRNA_028241	hsa_circ_0028241	chr12	exonic	ATXN2	0.006391718	0.499615783	1.5883582	up
hsa_circRNA_400095	hsa_circ_0092321	chr9	intronic	ZNF618	0.022564473	0.499615783	1.5846453	up
hsa_circRNA_007074	hsa_circ_0007074	chr1	exonic	YIPF1	0.041164698	0.499615783	1.5812649	up
hsa_circRNA_043614	hsa_circ_0043614	chr17	exonic	KRT14	0.032860267	0.499615783	1.5765257	up
hsa_circRNA_405086		chr12	exonic	LRRC43	0.025890515	0.499615783	1.5743094	up
hsa_circRNA_006290	hsa_circ_0006290	chr13	exonic	SLC7A1	0.041348694	0.499615783	1.5731505	up
hsa_circRNA_011717	hsa_circ_0011717	chr1	exonic	C1orf122	0.019863488	0.499615783	1.5703075	up
hsa_circRNA_406795		chr6	exonic	MTO1	0.004814004	0.499615783	1.5696956	up
hsa_circRNA_105044	hsa_circ_0001952	chrX	exonic	MPP1	0.011614067	0.499615783	1.5687106	up
hsa_circRNA_103471	hsa_circ_0067322	chr3	exonic	TMCC1	0.03804035	0.499615783	1.5669978	up
hsa_circRNA_015890	hsa_circ_0015890	chr1	exonic	CSRP1	0.038727162	0.499615783	1.5622244	up
hsa_circRNA_103809	hsa_circ_0072088	chr5	exonic	ZFR	0.048549567	0.499615783	1.5538255	up
hsa_circRNA_101511	hsa_circ_0007457	chr15	exonic	SPG11	0.009456106	0.499615783	1.552312	up
hsa_circRNA_024829	hsa_circ_0024829	chr11	exonic	ETS1	0.006799079	0.499615783	1.5432914	up
hsa_circRNA_104936	hsa_circ_0089033	chr9	exonic	PPP2R4	0.004848319	0.499615783	1.5413637	up
hsa_circRNA_406178		chr22	sense overlapping	CTA-292E10.6	0.040924422	0.499615783	1.5379459	up
hsa_circRNA_023828	hsa_circ_0023828	chr11	exonic	TENM4	0.031788947	0.499615783	1.5348674	up
hsa_circRNA_102206	hsa_circ_0045863	chr17	exonic	TNRC6C	0.009937467	0.499615783	1.5332035	up
hsa_circRNA_001805	hsa_circ_0001659	chr6	intronic	ARID1B	0.010956187	0.499615783	1.5307795	up
hsa_circRNA_102415	hsa_circ_0007376	chr19	exonic	MAP2K2	0.037667089	0.499615783	1.5291762	up
hsa_circRNA_003605	hsa_circ_0003605	chr10	exonic	ZMIZ1	0.039423163	0.499615783	1.5276411	up
hsa_circRNA_100441	hsa_circ_0007234	chr1	exonic	TRAF5	0.029650023	0.499615783	1.5240841	up
hsa_circRNA_100875	hsa_circ_0023397	chr11	exonic	NADSYN1	0.025298935	0.499615783	1.5232352	up
hsa_circRNA_103250	hsa_circ_0002657	chr22	exonic	ATXN10	0.00418255	0.499615783	1.5209281	up
hsa_circRNA_405722		chr19	exonic	CATSPERD	0.041018537	0.499615783	1.5191115	up
hsa_circRNA_404772		chr10	sense overlapping	UNC5B	0.009947528	0.499615783	1.5172142	up
hsa_circRNA_103963	hsa_circ_0001538	chr5	exonic	PAIP2	0.019822311	0.499615783	1.5168429	up
hsa_circRNA_405656		chr18	exonic	SPIRE1	0.046588452	0.499615783	1.5162693	up
hsa_circRNA_006668	hsa_circ_0006668	chr12	exonic	LETMD1	0.045684403	0.499615783	1.51528	up
hsa_circRNA_101045	hsa_circ_0025946	chr12	exonic	ANO6	0.019962826	0.499615783	1.5124775	up
hsa_circRNA_009435	hsa_circ_0009435	chr1	exonic	CEP104	0.032132414	0.499615783	1.5089374	up
hsa_circRNA_406127		chr20	exonic	GNAS-AS1	0.019536932	0.499615783	1.5057758	up
hsa_circRNA_000733	hsa_circ_0000733	chr17	sense overlapping	PRPF8	0.032685569	0.499615783	1.5046112	up
hsa_circRNA_081379	hsa_circ_0081379	chr7	exonic	ZKSCAN1	0.046815147	0.499615783	1.5023378	up
hsa_circRNA_103546	hsa_circ_0006517	chr3	exonic	LPP	0.003670382	0.499615783	4.9624886	down
hsa_circRNA_000441	hsa_circ_0001623	chr6	antisense	BACH2	0.024062795	0.499615783	4.6565074	down
hsa_circRNA_104004	hsa_circ_0074930	chr5	exonic	SLIT3	0.009518745	0.499615783	4.3713246	down

hsa_circRNA_100536	hsa_circ_0005379	chr10	exonic	GDI2	0.024695562	0.499615783	4.3190835	down
hsa_circRNA_001788	hsa_circ_0001788	chr8	exonic	PROSC	0.017835007	0.499615783	3.2240143	down
hsa_circRNA_104833	hsa_circ_0002191	chr9	exonic	C9orf3	0.043307778	0.499615783	3.196268	down
hsa_circRNA_000937	hsa_circ_0000937	chr19	exonic	BCKDHA	0.045187835	0.499615783	3.1939787	down
hsa_circRNA_101924	hsa_circ_0041150	chr17	exonic	RPH3AL	0.022996561	0.499615783	3.1771771	down
hsa_circRNA_402965		chr3	exonic	PCCB	0.018825871	0.499615783	3.1591999	down
hsa_circRNA_000466	hsa_circ_0001745	chr7	antisense	LINC-PINT	0.015231971	0.499615783	3.1354324	down
hsa_circRNA_062556	hsa_circ_0062556	chr22	exonic	CHCHD10	0.040099626	0.499615783	3.0828941	down
hsa_circRNA_005133	hsa_circ_0005133	chr6	exonic	DDR1	0.039196111	0.499615783	2.8751048	down
hsa_circRNA_012123	hsa_circ_0012123	chr1	exonic	ATP6V0B	0.01625424	0.499615783	2.7735782	down
hsa_circRNA_401015		chr12	exonic	SLC25A3	0.03342162	0.499615783	2.7657968	down
hsa_circRNA_405080		chr12	sense overlapping	RP13-941N14.1	0.040009216	0.499615783	2.7550538	down
hsa_circRNA_056159	hsa_circ_0056159	chr2	exonic	IL1RN	0.023679538	0.499615783	2.6426649	down
hsa_circRNA_103384	hsa_circ_0065898	chr3	exonic	VPRBP	0.034970381	0.499615783	2.6369745	down
hsa_circRNA_001238	hsa_circ_0000429	chr12	sense overlapping	CEP83	0.032831335	0.499615783	2.5316617	down
hsa_circRNA_000186	hsa_circ_0000186	chr1	intronic	MIA3	0.030695331	0.499615783	1.9983032	down
hsa_circRNA_040097	hsa_circ_0040097	chr16	exonic	WWP2	0.044052438	0.499615783	1.9704381	down
hsa_circRNA_081055	hsa_circ_0081055	chr7	exonic	COL1A2	0.049933107	0.499615783	1.9649983	down
hsa_circRNA_000850	hsa_circ_0000850	chr18	exonic	ME2	0.036352919	0.499615783	1.9039714	down
hsa_circRNA_405422		chr15	sense overlapping	NR2F2-AS1	0.022931715	0.499615783	1.8977825	down
hsa_circRNA_405477		chr16	intronic	LCAT	0.030503008	0.499615783	1.8959592	down
hsa_circRNA_403650		chr6	exonic	MRAP2	0.031187279	0.499615783	1.8813667	down
hsa_circRNA_029830	hsa_circ_0029830	chr13	exonic	PAN3	0.023757924	0.499615783	1.8793685	down
hsa_circRNA_059354	hsa_circ_0059354	chr20	exonic	RASSF2	0.010238128	0.499615783	1.8781427	down
hsa_circRNA_048584	hsa_circ_0048584	chr19	exonic	SIRT6	0.044518919	0.499615783	1.8482887	down
hsa_circRNA_100073	hsa_circ_0010358	chr1	exonic	UBR4	0.013701938	0.499615783	1.8279876	down
hsa_circRNA_406142		chr21	exonic	CRYZL1	0.038515296	0.499615783	1.8244022	down
hsa_circRNA_407325		chrX	sense overlapping	RP11-41L14.1	0.023194467	0.499615783	1.8098288	down
hsa_circRNA_049472	hsa_circ_0049472	chr19	exonic	PRKCSH	0.026168892	0.499615783	1.8054976	down
hsa_circRNA_049241	hsa_circ_0049241	chr19	exonic	ICAM1	0.001858104	0.499615783	1.8015372	down
hsa_circRNA_007215	hsa_circ_0007215	chr4	sense overlapping	RGS12	0.031860293	0.499615783	1.7952488	down
hsa_circRNA_103633	hsa_circ_0069681	chr4	exonic	FRYL	0.029707353	0.499615783	1.7948172	down
hsa_circRNA_090682	hsa_circ_0090682	chrX	exonic	HUWE1	0.036871181	0.499615783	1.7881297	down
hsa_circRNA_008077	hsa_circ_0008077	chrX	exonic	PRRG1	0.023831492	0.499615783	1.7873646	down
hsa_circRNA_403202		chr4	exonic	ELOVL6	0.021345856	0.499615783	1.7844566	down
hsa_circRNA_006691	hsa_circ_0006691	chr16	exonic	WDR59	0.018525504	0.499615783	1.7823156	down
hsa_circRNA_031809	hsa_circ_0031809	chr14	exonic	NEMF	0.018139126	0.499615783	1.7806277	down
hsa_circRNA_069059	hsa_circ_0069059	chr4	exonic	EVC2	0.004663237	0.499615783	1.776311	down
hsa_circRNA_100621	hsa_circ_0018814	chr10	exonic	PPP3CB	0.033051121	0.499615783	1.7655024	down
hsa_circRNA_405752		chr19	exonic	SUGP2	0.049505665	0.499615783	1.7642027	down
hsa_circRNA_010096	hsa_circ_0010096	chr1	exonic	FBLIM1	0.030511309	0.499615783	1.7584738	down
hsa_circRNA_014234	hsa_circ_0014234	chr1	exonic	S100A2	0.016641323	0.499615783	1.7565815	down
hsa_circRNA_072303	hsa_circ_0072303	chr5	exonic	LIFR	0.013607299	0.499615783	1.7539015	down
hsa_circRNA_102955	hsa_circ_0007713	chr2	exonic	UBE2F	0.028529988	0.499615783	1.7505659	down
hsa_circRNA_000166	hsa_circ_0000512	chr14	sense overlapping	RPPH1	0.003958728	0.499615783	1.7371844	down
hsa_circRNA_407293		chrX	exonic	OPHN1	0.01184914	0.499615783	1.7329091	down
hsa_circRNA_082275	hsa_circ_0082275	chr7	exonic	TNPO3	0.005226257	0.499615783	1.7270373	down
hsa_circRNA_103818	hsa_circ_0072279	chr5	exonic	NUP155	0.018749122	0.499615783	1.7110621	down
hsa_circRNA_001484	hsa_circ_0000701	chr16	sense overlapping	CHD9	0.010407719	0.499615783	1.710493	down
hsa_circRNA_104504	hsa_circ_0082600	chr7	exonic	TRIM24	0.047580335	0.499615783	1.7059794	down
hsa_circRNA_104700	hsa_circ_0005273	chr8	exonic	PTK2	0.021001464	0.499615783	1.7041422	down
hsa_circRNA_103826	hsa_circ_0072380	chr5	exonic	ZNF131	0.04656445	0.499615783	1.7010271	down
hsa_circRNA_061554	hsa_circ_0061554	chr21	exonic	CRYZL1	0.048809403	0.499615783	1.6963302	down
hsa_circRNA_002261	hsa_circ_0002261	chr10	exonic	FAM21A	0.010871631	0.499615783	1.6934996	down
hsa_circRNA_059104	hsa_circ_0059104	chr2	exonic	THAP4	0.019489994	0.499615783	1.6899265	down
hsa_circRNA_101484	hsa_circ_0007489	chr15	exonic	INO80	0.037080389	0.499615783	1.6848882	down
hsa_circRNA_404788		chr10	exonic	LIPA	0.011711639	0.499615783	1.6749865	down

hsa_circRNA_102625	hsa_circ_0052760	chr2	exonic	NBAS	0.034153334	0.499615783	1.669633	down
hsa_circRNA_104642	hsa_circ_0084678	chr8	exonic	CSPP1	0.017631326	0.499615783	1.6694338	down
hsa_circRNA_404473		chr1	antisense	XLOC_000133	0.021366276	0.499615783	1.6678426	down
hsa_circRNA_104725	hsa_circ_0007787	chr8	exonic	RECQL4	0.040131698	0.499615783	1.6605465	down
hsa_circRNA_002009	hsa_circ_0002009	chr12	exonic	ITFG2	0.000573428	0.499615783	1.6595806	down
hsa_circRNA_100069	hsa_circ_0002733	chr1	exonic	PLEKHM2	0.041364486	0.499615783	1.6595681	down
hsa_circRNA_001096	hsa_circ_0000866	chr19	antisense	RPS15	0.010896145	0.499615783	1.6480562	down
hsa_circRNA_406445		chr4	intronic	EVC	0.028811395	0.499615783	1.6471235	down
hsa_circRNA_026634	hsa_circ_0026634	chr12	exonic	PCBP2	0.009415589	0.499615783	1.646467	down
hsa_circRNA_057362	hsa_circ_0057362	chr2	exonic	COL3A1	0.038141199	0.499615783	1.6448036	down
hsa_circRNA_400732		chr11	exonic	QSER1	0.04182965	0.499615783	1.6407624	down
hsa_circRNA_405985		chr2	sense overlapping	LOC100506124	0.012666623	0.499615783	1.6383866	down
hsa_circRNA_102805	hsa_circ_0056146	chr2	exonic	POLR1B	0.015540259	0.499615783	1.6303538	down
hsa_circRNA_104593	hsa_circ_0083964	chr8	exonic	ASH2L	0.043665278	0.499615783	1.6298865	down
hsa_circRNA_000536	hsa_circ_0000536	chr14	sense overlapping	LOC100506499	0.040157963	0.499615783	1.6256932	down
hsa_circRNA_100726	hsa_circ_0002456	chr10	exonic	DOCK1	0.033642413	0.499615783	1.6246851	down
hsa_circRNA_101450	hsa_circ_0033598	chr14	exonic	PACS2	0.01671127	0.499615783	1.6231206	down
hsa_circRNA_008404	hsa_circ_0008404	chr14	exonic	AHSA1	0.014209333	0.499615783	1.6170342	down
hsa_circRNA_062557	hsa_circ_0062557	chr22	exonic	CHCHD10	0.040662772	0.499615783	1.6086926	down
hsa_circRNA_092416	hsa_circ_0000593	chr15	exonic	MGA	0.019408529	0.499615783	1.6082662	down
hsa_circRNA_100753	hsa_circ_0002969	chr11	exonic	TRIM6	0.047485161	0.499615783	1.6081471	down
hsa_circRNA_406013		chr2	exonic	SF3B1	0.032758248	0.499615783	1.6045768	down
hsa_circRNA_404254		chr9	exonic	BRINP1	0.016449881	0.499615783	1.6044089	down
hsa_circRNA_102484	hsa_circ_0005571	chr19	exonic	IFI30	0.037548934	0.499615783	1.6038758	down
hsa_circRNA_104989	hsa_circ_0090142	chrX	exonic	POLA1	0.004461952	0.499615783	1.6036017	down
hsa_circRNA_083182	hsa_circ_0083182	chr7	exonic	NCAPG2	0.03940374	0.499615783	1.6018373	down
hsa_circRNA_100121	hsa_circ_0005174	chr1	exonic	SNHG12	0.008550402	0.499615783	1.5982556	down
hsa_circRNA_006149	hsa_circ_0006149	chr19	exonic	KEAP1	0.042819953	0.499615783	1.5913818	down
hsa_circRNA_064170	hsa_circ_0064170	chr3	exonic	ARPC4	0.012239271	0.499615783	1.5891078	down
hsa_circRNA_100024	hsa_circ_0009135	chr1	exonic	NPHP4	0.039736456	0.499615783	1.5875017	down
hsa_circRNA_103337	hsa_circ_0065052	chr3	exonic	ZDHHC3	0.009745316	0.499615783	1.5871498	down
hsa_circRNA_000931	hsa_circ_0001045	chr2	intronic	MRPS5	0.028380074	0.499615783	1.5864471	down
hsa_circRNA_100445	hsa_circ_0016404	chr1	exonic	TATDN3	0.046034315	0.499615783	1.5824984	down
hsa_circRNA_020924	hsa_circ_0020924	chr11	exonic	RHOG	0.040157847	0.499615783	1.5800135	down
hsa_circRNA_406350		chr3	exonic	IFT122	0.019527964	0.499615783	1.5786064	down
hsa_circRNA_008702	hsa_circ_0008702	chr1	exonic	GNB1	0.049314446	0.499615783	1.5771817	down
hsa_circRNA_101865	hsa_circ_0000715	chr16	exonic	PHLPP2	0.030416836	0.499615783	1.5758656	down
hsa_circRNA_092454	hsa_circ_0000863	chr19	sense overlapping	PRSS57	0.029784069	0.499615783	1.5756113	down
hsa_circRNA_404957		chr12	exonic	NDUFA9	0.043569719	0.499615783	1.5746871	down
hsa_circRNA_406491		chr4	exonic	PRKG2	0.027319079	0.499615783	1.5740703	down
hsa_circRNA_007148	hsa_circ_0007148	chr3	exonic	FNDC3B	0.01694737	0.499615783	1.5704583	down
hsa_circRNA_104469	hsa_circ_0082140	chr7	exonic	SND1	0.038760638	0.499615783	1.5663756	down
hsa_circRNA_001572	hsa_circ_0001572	chr6	sense overlapping	PRPF4B	0.047054118	0.499615783	1.5661034	down
hsa_circRNA_102450	hsa_circ_0006877	chr19	exonic	LDLR	0.018084192	0.499615783	1.5566538	down
hsa_circRNA_400090	hsa_circ_0092341	chr6	intronic	C6orf132	0.03557133	0.499615783	1.5560451	down
hsa_circRNA_083932	hsa_circ_0083932	chr8	exonic	PROSC	0.01831233	0.499615783	1.5511611	down
hsa_circRNA_104728	hsa_circ_0086242	chr9	exonic	RFX3	0.030472419	0.499615783	1.5510095	down
hsa_circRNA_104959	hsa_circ_0089490	chr9	exonic	CAMSAP1	0.016789261	0.499615783	1.5499954	down
hsa_circRNA_405732		chr19	exonic	RGL3	0.018512961	0.499615783	1.5484281	down
hsa_circRNA_403788		chr7	exonic	SKAP2	0.004242431	0.499615783	1.548388	down
hsa_circRNA_101115	hsa_circ_0027774	chr12	exonic	METAP2	0.044381566	0.499615783	1.5446852	down
hsa_circRNA_065926	hsa_circ_0065926	chr3	exonic	RAD54L2	0.025097909	0.499615783	1.5442972	down
hsa_circRNA_404245		chr9	exonic	ZNF483	0.034322677	0.499615783	1.5427621	down
hsa_circRNA_063313	hsa_circ_0063313	chr22	exonic	DDX17	0.012347518	0.499615783	1.542562	down
hsa_circRNA_400710		chr11	exonic	GALNT18	0.018609726	0.499615783	1.5410804	down
hsa_circRNA_028671	hsa_circ_0028671	chr12	exonic	TAOK3	0.044066808	0.499615783	1.5410133	down
hsa_circRNA_074537	hsa_circ_0074537	chr5	exonic	RPS14	0.048564224	0.499615783	1.5383984	down

hsa_circRNA_101465	hsa_circ_0034189	chr15	exonic	OCA2	0.030564651	0.499615783	1.5376547	down
hsa_circRNA_064277	hsa_circ_0064277	chr3	exonic	SEC13	0.038937167	0.499615783	1.536243	down
hsa_circRNA_405010		chr12	exonic	COPZ1	0.017215911	0.499615783	1.535249	down
hsa_circRNA_001047	hsa_circ_0001047	chr2	exonic	NCAPH	0.048984124	0.499615783	1.5342677	down
hsa_circRNA_101145	hsa_circ_0028198	chr12	exonic	ANAPC7	0.037608242	0.499615783	1.5333926	down
hsa_circRNA_003300	hsa_circ_0003300	chrX	exonic	LRCH2	0.038714916	0.499615783	1.5287945	down
hsa_circRNA_405567		chr17	intronic	RAD51L3-RFFL	0.040335884	0.499615783	1.527817	down
hsa_circRNA_104839	hsa_circ_0087643	chr9	exonic	CDC14B	0.033417018	0.499615783	1.5272609	down
hsa_circRNA_101633	hsa_circ_0036629	chr15	exonic	PDE8A	0.010416946	0.499615783	1.5229035	down
hsa_circRNA_407287		chrX	sense overlapping	RP11-348F1.3	0.015138446	0.499615783	1.5154481	down
hsa_circRNA_406673		chr5	intronic	SPOCK1	0.025997487	0.499615783	1.5154163	down
hsa_circRNA_104017	hsa_circ_0004004	chr5	exonic	ERGIC1	0.000993711	0.499615783	1.5130565	down
hsa_circRNA_101785	hsa_circ_0038821	chr16	exonic	XPO6	0.02097256	0.499615783	1.5129463	down
hsa_circRNA_039816	hsa_circ_0039816	chr16	exonic	SLC9A5	0.048380832	0.499615783	1.5110716	down
hsa_circRNA_406187		chr22	sense overlapping	CPSF1P1	0.04749148	0.499615783	1.5103471	down
hsa_circRNA_100362	hsa_circ_0000142	chr1	exonic	CCT3	0.0010325	0.499615783	1.5090338	down
hsa_circRNA_001430	hsa_circ_0001516	chr5	exonic	CTD-2215E18.1	0.033986655	0.499615783	1.5078682	down
hsa_circRNA_100944	hsa_circ_0024143	chr11	exonic	DYNC2H1	0.0059244	0.499615783	1.5072283	down
hsa_circRNA_079276	hsa_circ_0079276	chr7	exonic	ACTB	0.041132902	0.499615783	1.5056931	down
hsa_circRNA_401717		chr17	exonic	ZNF286A	0.0350921	0.499615783	1.50547	down
hsa_circRNA_000285	hsa_circ_0000285	chr11	exonic	HIPK3	0.009949908	0.499615783	1.5009228	down

Among 226 differentially expressed circRNAs (fold change ≥1.5, *P*-value <0.05 and FDR <0.05), 88 circRNAs were up-regulated and 138 circRNAs were down-regulated. Alias: the circRNA ID in circBase (http://www.circbase.org).

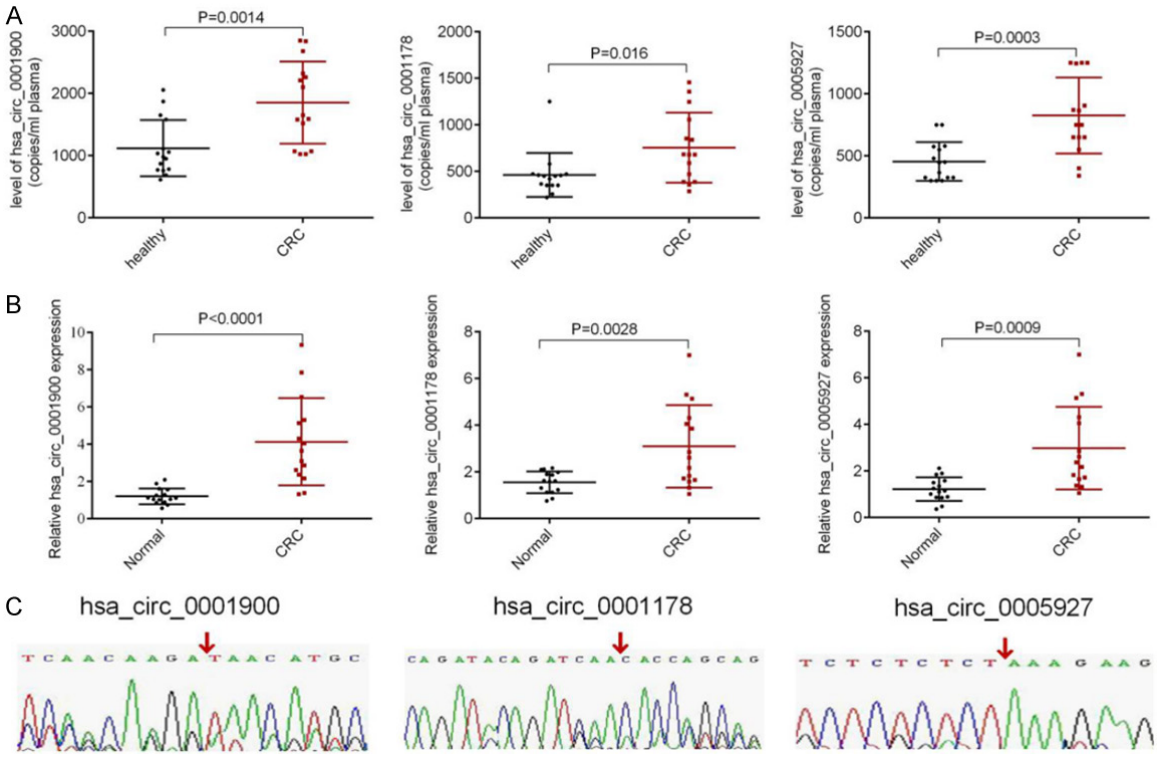

Figure S2. The quantification of the three candidate circRNAs in CRC tissues and plasma. A. qRT-PCR showed the absolute RNA levels of hsa_circ_0001900, hsa_circ_0001178 and hsa_circ_0005927 in 15 CRC and 15 healthy plasma. B. qRT-PCR showed the relative RNA levels of hsa_circ_0001900, hsa_circ_0001178 and hsa_circ_0005927 in 15 paired CRC and normal tissues. GAPDH was used as the internal control. C. Sanger sequencing showing the back-spliced events of candidate circRNAs.

Table S4. The performance of three candidate circRNAs and CircPanel for the diagnosis of CRC

Groups	Cut off	AUC (95% CI)	Sensitivity (%)	Specificity (%)	*P* value#
hsa_circ_0001900	1883 copies/ml	0.722 (95% CI 0.656-0.781)	67.65%	68.18%	<0.0001
hsa_circ_0001178	582 copies/ml	0.718 (95% CI 0.652-0.778)	71.57%	71.82%	0.0001
hsa_circ_0005927	578 copies/ml	0.784 (95% CI 0.722-0.837)	63.73%	80.00%	0.0017
CircPanel	0.5	0.859 (95% CI 0.805-0.903)	72.55%	82.73%	NA

#, The *P* values indicate the statistical significance for the differences of AUC as compared with CircPanel.

Table S5. The performance of CircPanel for the diagnosis of CEA-negative CRC

Groups	AUC (95% CI)	Sensitivity (%)	Specificity (%)
CRC vs. Non-CRC	0.846 (95% CI 0.783-0.897)	72.13%	82.73%
CRC vs. Healthy	0.861 (95% CI 0.792-0.913)	72.17%	85.00%
CRC vs. precancerous	0.805 (95% CI 0.709-0.881)	83.61%	70.00%